J Mater Sci (2006) 41:6245–6255
DOI 10.1007/s10853-006-0494-9

Design and modeling of multiple layered TBC system with high reflectance

Dongmei Wang · Xiao Huang · Prakash Patnaik

Received: 13 August 2004 / Accepted: 23 September 2005 / Published online: 12 August 2006

Abstract Ceramic thermal barrier coatings (TBCs) are playing an increasingly critical role in advanced gas turbine engines due to their ability to sustain further increases in operating temperatures. However, these increases in temperature could raise considerable issues associated with increased radiative heat transfer into the TBC systems. This study was conducted to design a ceramic based multiple layered TBC system with high reflectance to radiation. Mathematical modeling was used to calculate the potential temperature reduction on the substrate surface when the multiple layered TBC is applied. The result of the simulation shows that a temperature reduction up to 90 °C is possible when utilizing the designed multiple layered TBC coatings.

Introduction

Thermal barrier coatings (TBCs) are applied to metallic substrates to reduce the metal surface temperature. The currently preferred TBC material for gas turbine engine applications is yttria partially stabilized zirconia (YPSZ). Zirconium oxide has a lower intrinsic thermal conductivity, an expansion coefficient more comparable to the metal substrate than other ceramics such as Al_2O_3, and exhibits good erosion resistance. However, in order to stabilize the cubic or tetragonal structure, yttria (Y_2O_3) is added into zirconia, preventing the phase transformation to monoclinic ZrO_2. This stabilized zirconia exhibits increased toughness and strength, and has lower thermal conductivity, than pure zirconia. The addition of yttria creates more O^{2-} vacancies in the ionic lattice of the ZrO_2 structure in order to maintain electrical neutrality. The increased vacancies strongly scatter phonons by virtue of both varied mass and missing interatomic linkage [1].

Continuous development and advancement in TBCs to improve the performance, particularly in reduction of thermal conductivity, are required in order to enable further increases in turbine inlet temperature, reductions in air cooling requirements and improvements in component durability. In the past, extensive research has focused on modifying the composition of new TBC materials and processing methods to reduce thermal conductivity. For example, additions of erbia, nickel oxide, neodymia and ytterbia etc. into YPSZ have been studied, achieving further reduction in thermal conductivity [2]. Modification of the coatings into a zig-zag layered structure has been shown to offer high impedance to heat flow and provide improved thermal and mechanical properties [3]. However, due to high temperature instability, sintering effect and phase transformation to monoclinic structure [4–6], YPSZ is limited to a maximum operating temperature of 1200 °C [5]. New generation TBC materials have been studied, of which lanthanum zirconate ($La_2Zr_2O_7$) seems to be most promising. It has phase stability up to its melting temperature, similar thermal expansion to

D. Wang · X. Huang (✉)
Department of Mechanical and Aerospace Engineering, Carleton University, Ottawa, Canada
e-mail: xhuang@mae.carleton.ca

P. Patnaik
Structures, Materials and Propulsion Laboratory, Institute for Aerospace Research, National Research Council, Ottawa, Canada
e-mail: prakash.patnaik@nrc.ca

that of zirconia, and better thermal insulation properties than those of the more commonly used zirconia based TBC materials [7].

Surprisingly, there has been only very limited research into microstructure and process modifications for the purpose of reducing thermal radiation transport through the TBC system to the metallic substrate. The zirconia based ceramic materials are transparent or translucent to certain radiation wavelength. As shown in Fig. 1, the infrared radiative properties of single crystal yttria-stabilized zirconia were given [8]. In this figure, the spectral hemispherical transmittance, reflectance and emittance of single crystal 13.5YSZ specimens of various thicknesses at room temperature were measured. As seen in figure 1, in region I (0.3–5 μm) the material exhibits a high transmittance with low absorption, and in region II (5–10 μm) the material exhibits partial absorption and partial transmission. In region III, the material shows an opposite trend as compared to what is seen in region I. While no scattering is observed in single crystal zirconia, scatting is expected in zirconia based polycrystalline TBC. The extent of the scattering is dependent on the microstructure, particularly imperfections, in the coating. This could increases the reflection since transmitted radiation will be reduced accordingly. In a previous

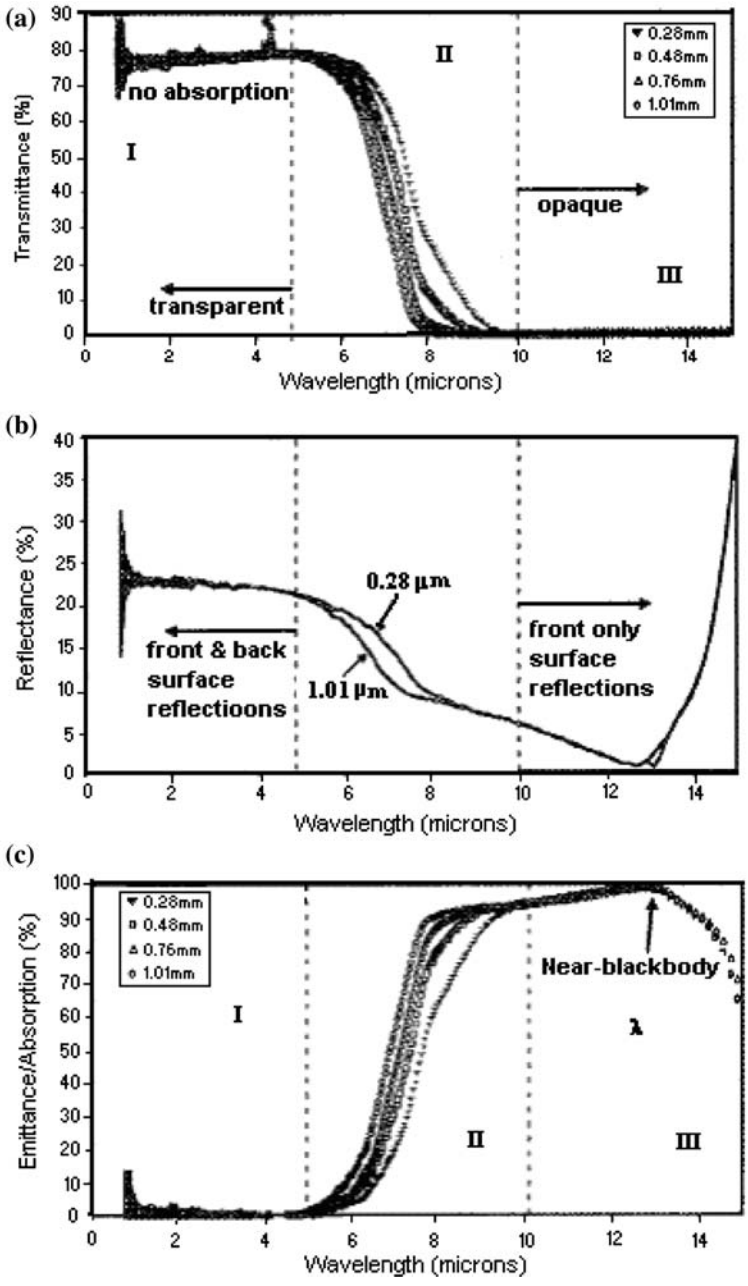

Fig. 1 Room-temperature (**a**) hemispherical transmittance, (**b**) reflectance, and (**c**) emittance/absorptance along (100) direction of single crystal 13.5YSZ specimens with various thicknesses [8]

mathematical simulation conducted by R. Siegel [9], the thermal radiation effect on temperature distribution in turbine engine TBCs was modeled based on a plasma sprayed coating. Scattering was considered as a scattering coefficient of 10,000 m^{-1} was used. According to this calculation, the temperature increase on the metallic substrate resulting from radiation effects was as high as 50 °C as compared to that of an opaque coating, as shown in Fig. 2.

In order to effectively reduce thermal radiation transport through TBC systems, research has been carried out with emphasis on increasing the photon scattering within the coating and the coating's reflectivity. A layered TBC structure, produced using EB-PVD, was able to reduce thermal radiation by increasing scattering defects such as boundaries between multiple layers [10]. Increasing the density of scattering defects such as microcracks and pores within the coating has also been reported as another efficient way of reducing thermal radiation [3]. Recently, a new multiple layered coating structure was patented [11]. In this structure, highly reflective metallic layers were embedded within the protective ceramic coatings for the purpose of reducing the radiation heat transport. A computational analysis showed a 12–24% reduction in the net heat flux for a ceramic coating containing a single metallic layer as compared to a ceramic coating without a reflective metallic layer. The use of metal reflective layers in a TBC may, however, be expected to be problematic due to the thermal expansion coefficient mismatch between the metallic and ceramic materials, poor adhesion of the ceramic material to the metal, and high thermal conductivity inherent to metals. Additionally, the radiation reflection may be reduced if the surface of the metallic layers is not smooth enough when embedded in ceramics.

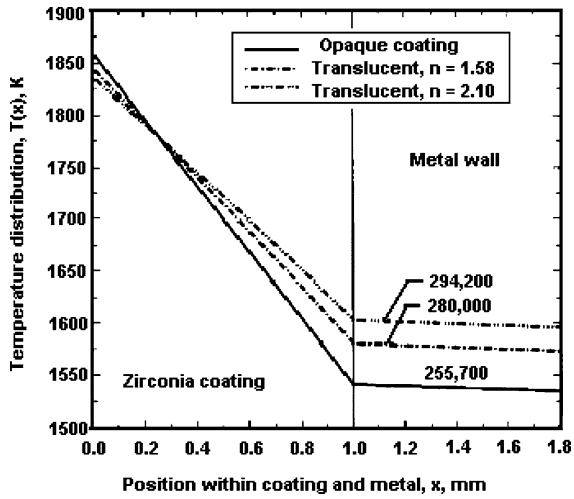

Fig. 2 Temperature distributions in a zirconia thermal barrier coating on the wall of a combustor compared with an opaque thermal barrier coating [9]

The present study was undertaken to develop a new multiply layered TBC system based solely on ceramic materials. The objective of this research is to design a system that is capable of reflecting radiation with the wavelength in the range of 0.45–5 μm. The preliminary design and mathematical simulation are detailed in the following sections.

Design of multiple layered TBC system with high reflectance

The radiation transport through TBCs to the metal component originates from two sources [9]: (1) external radiation from hot gases or soot (if existing), which is directly incident onto the coating surface and transmitted to the substrate; and (2) internal radiation emission within the hot coating itself when heated by convection from combustion gases, conduction within the coating system or absorption of external and internal radiation. To achieve a significant reduction in both external and internal radiation, and effectively reduce the temperature increase on the substrate caused by radiation, a multiple layered high reflective coating system is required.

The multi-layer TBC system (Fig. 3) consists of a single top layer (S) with low thermal conductivity and low refractive index, a set of high reflectance multiple layered ceramic stacks (M) that are designed to cover radiation in the wavelength range of 0.45–5 μm, a bond coat and the metal substrate. The choice of wavelength range is based on the fact that more than 90% of radiation is within this range at typical gas temperature of 1700–2000 K (Fig. 4).

There are three considerations for the S layer design. First, the emissive power in a medium is proportional to the square of the refractive index of the

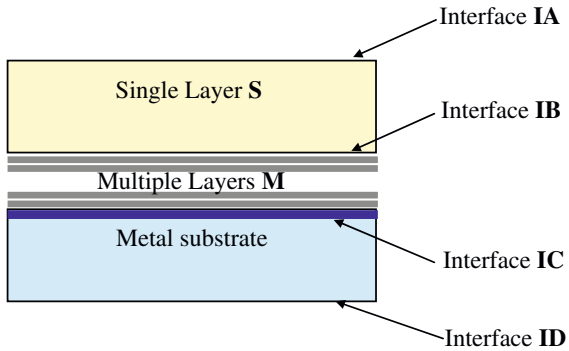

Fig. 3 Multiple layered TBC system with high reflectance

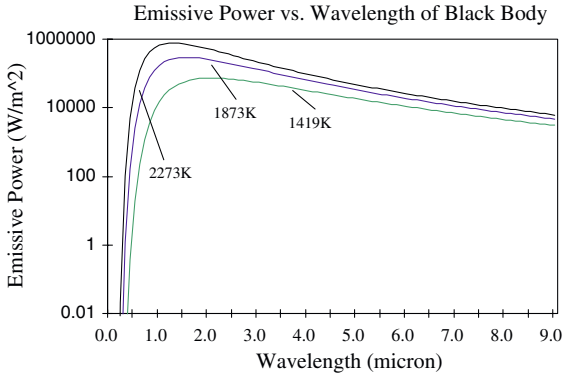

Fig. 4 Spectral distribution of blackbody emissive power at different temperatures

material [12]. Therefore, if the refractive index of S layer is high, the internal radiation emitted by S layer will be high. A high refractive index can also increase internal reflection at interface IA and result in increased radiation reflected back into the coatings, thereby increasing the temperature of the coating system. Therefore, to suppress the radiation from inside the coatings and to reduce the internal reflection at interface IA, the refractive index of the S layer should be as low as possible. Secondly, the photon scattering coefficient of the S layer should be as low as possible so that the reflected radiation from high reflectance multiple layers will not be scattered back. Finally, since the temperature at interface IB and within high reflectance multiple layered stacks should be as low as possible so that the radiation emission from M layer is negligible, the S layer, if placed on top of M layer, should have lower thermal conductivity. However, these parameters shall be optimized systematically based on the simulations of temperature distribution through the designed system.

Within the multiple stacks M, each stack is designed to reflect a targeted range of wavelength. A broadband reflection for the required wavelength range can be obtained using sufficient number of stacks. To achieve high reflectance for each wavelength range, each stack must have multiple layers of ceramic materials with alternating high and low refractive indices and the optical thickness of each layer must be equal to a quarter wavelength in order to meet the condition of multiple-beam interference. Considering that the radiation with shorter wavelength will be scattered more strongly than longer wavelength within the coating, the stack reflecting shorter wavelength range is therefore arranged to the top of the multiple layer stacks, and the stack reflecting longest wavelength range is at the very bottom of the multiple layered stacks S. Using this arrangement, undesirable scattering is reduced as such to ensure higher reflection. Since thin film coating scattering is mainly caused by defects such as interface and pores within the coating, the coating process and coating material will be investigated to obtain an ideal structure in order to have high reflectance, high strain tolerance and lower thermal conductivity at the same time. Figure 5 shows schematically how the radiation is reflected and transmitted by these multiple layered stacks.

The physical thickness of each layer in one stack can be calculated using [13]:

$$d_{\mathrm{H}}(\lambda) = \lambda/(4n_{\mathrm{H}}) \tag{1}$$

$$d_{\mathrm{L}}(\lambda) = \lambda/(4n_{\mathrm{s}}) \tag{2}$$

where d_{H} and d_{L} are thicknesses for the alternating layers within the stack, and n_{H} and n_{L} are the refractive indices of the alternating layers. H denotes layer with high reflective index and L denotes layer with low reflective index. λ is the radiation wavelength.

Assuming that the absorption of and scattering to the radiation in the high reflectance stacks are negligible, then the reflectance for one wavelength range is given by:

$$R = \left(\frac{\eta_0 B - C}{\eta_0 B + C}\right)\left(\frac{\eta_0 B - C}{\eta_0 B + C}\right) \tag{3}$$

where

$$\begin{bmatrix} B \\ C \end{bmatrix} = \left(\prod_{r=1}^{q} \begin{bmatrix} \cos\delta_r & (i\sin\delta_r)/\eta_r \\ i\eta_r \sin\delta_r & \cos\delta_r \end{bmatrix}\right)\begin{bmatrix} 1 \\ \eta_m \end{bmatrix} \tag{4}$$

and

$$\delta_r = 2\pi n_r d_r \cos\theta_r/\lambda \tag{5}$$

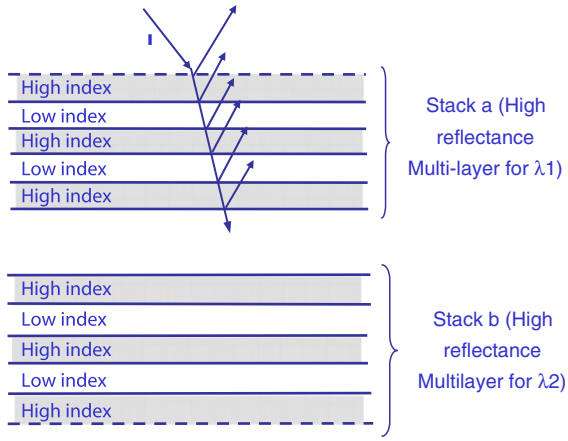

Fig. 5 Schematic diagram of high reflectance multiple layered TBC structure

and η_0, η_r and η_m are the optical admittances for incident medium, multiple layers M and substrate, respectively. θ_r is the incident angle, d_r is the layer thickness, n_r is the refractive index of each layer, r is the layer number and q is the total number of layers within a stack.

For p-wave, $\eta_p = \frac{2.6544\times10^{-3}n}{\cos\theta}$ and for s-wave, $\eta_s = 2.6544 \times 10^{-3} n \cos\theta$.

Under normal incidence condition, the reflectance in air or free space for one wavelength range is expressed as:

$$R \approx 1 - 4\left(\frac{n_{\mathrm{L}}}{n_{\mathrm{H}}}\right)^{2p}\frac{n_m}{n_{\mathrm{H}}^2} \tag{6}$$

The width of the high-reflectance wavelength zone is:

$$\Delta\lambda = \frac{2\lambda}{\pi}\sin^{-1}\left(\frac{n_{\mathrm{H}} - n_{\mathrm{L}}}{n_{\mathrm{H}} + n_{\mathrm{L}}}\right) \tag{7}$$

where n_m is the refractive index of substrate.

Assuming $n_{\mathrm{L}} = 1.5$, $n_m = 2.2$, and $n_{\mathrm{H}} = 2.2$, the number of stacks and layers as well as the physical thickness of each layer can be calculated. Under an isotropic hemispherical incident condition, for a multilayered coating design consisting of 10 stacks and a total of 79 layers the hemispherical spectral reflectance within the wavelength range of 0.45–5 μm is calculated by integrating Eq. 3 from 0 to 180° using the method detailed in Ref. [12]. From the calculation results given in Fig. 6, the average hemispherical reflectance is above 80% for wavelength range of 1–4.5μm.

In the computation of hemispherical spectral reflectance, the scattering effect and absorption are neglected. In fact, TBCs deposited by either plasma sprayed or EB-PVD always exhibits higher scattering due to the splats or columnar characteristics of their microstructures. These scattering will affect the coherent constructive interference and reduce the effective reflectance. Thus, in the analytical simulation, the hemispherical reflectance of the multiple layered coatings is conservatively assumed to be 50% to take into consideration of the scattering effect. An accurate calculation of the effect of the scattering on the hemispherical reflectance of multiple layered coatings is currently being undertaken and will be presented in future publication.

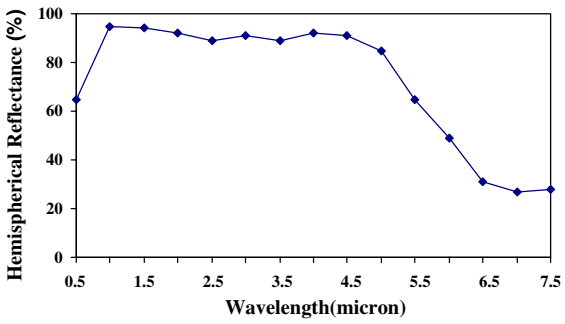

Fig. 6 Calculated hemispherical reflectance of 10 stacks with 79 layers

Analytical simulation for the high reflectance multiple layered TBC system

Using the multiple layered design described above, a one-dimensional heat transfer model was established by the authors and the two-flux method [12] used to analytically simulate the heat transfer through the multiple layered TBC system with high reflectance.

A translucent multiple layered ceramic TBC system within the environment of high temperature is shown in Fig. 7. The gas temperatures on both sides of the wall are T_{H} (hot side) and T_{L} (cool side), and under thermal equilibrium state, these temperatures remain constant. At the hot side, the heat is transferred into the TBC system by external convection with the convection coefficient h_{H}, and by external radiation from hot gases incident on the coating surface IA with the radiation flux $q_{r\mathrm{H}}$. At the cool side of the metal wall, the temperature is reduced by cold gas convection with the convection coefficient h_{L} and by radiation emitting from the metal surface to the surrounding environment with the radiation flux $q_{r\mathrm{L}}$. Under steady state condition the total heat flux through the layers is time independent.

Additional assumptions made are as follows:

- An EB-PVD coating is used, the scattering effect is assumed to be equivalent to or less than plasma sprayed coating since it doesn't contain lateral splat interfaces. A scattering efficient of 10,000 m^{-1} given in Ref. [9] is used for both single layer S and multiple layered stacks M.
- The absorption coefficients of single layer S and multiple layered high-reflectance stacks M are assumed to be the same as given in Ref. [9].
- The refractive index does not change with wavelength.
- The gray layer assumption is used in this analysis.
- For simplicity, the multiple layered stacks will be considered as a single layer with an effective reflectance of 50%.
- The thermal conductivity of multiple layered stacks M is calculated using $1/k_j = 1/k_{\mathrm{H}} + 1/k_{\mathrm{L}}$.

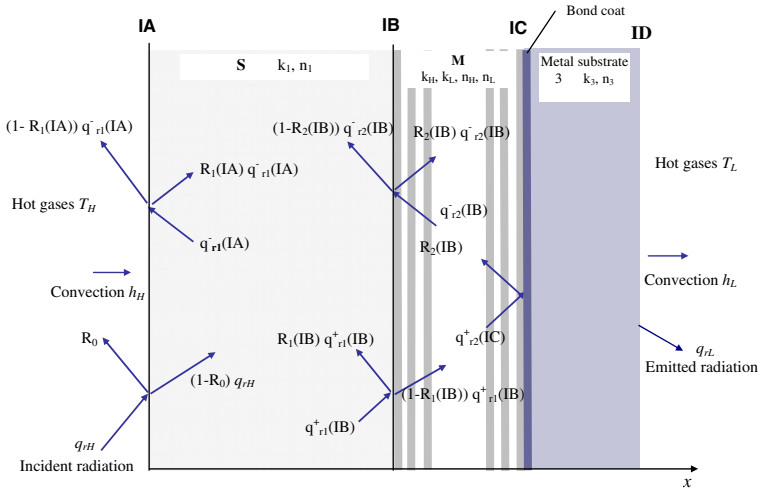

Fig. 7 Schematics of heat transfer for the high reflectance multiple layered TBC system within the environment of high temperature

- A worse case scenario is assumed when considering the effective refractive index of the multiple layered stacks and a value of 2.2 is used [9].
- Black body gas is assumed.
- Hemispherical/isotropic radiation incidence is considered.

Within the transparent coatings, the radiation heat flux components can be obtained by solving two-flux equations [12] expressed as:

$$\frac{1}{K_j}\frac{dq_{rj}}{dx_j} = (1-\Omega_j)[4n_j^2\sigma T_j^4(x) - G_j(x_j)] \tag{8}$$

$$\frac{1}{K_j}\frac{dG_j}{dx_j} = -3q_{rj} \tag{9}$$

$$\Omega_j = \sigma_j/K_j \tag{10}$$

where $j = 1$ for the single layer S and $j = 2$ for the high-reflectance multiple layered stacks M.

$$G_j = 2(q_{rj}^+ + q_{rj}^-) \tag{11}$$

$$q_{rj} = q_{rj}^+ - q_{rj}^- \tag{12}$$

where $q^+{}_{rj}$ and $q^-{}_{rj}$ are the radiation heat fluxes in positive and negative directions, respectively, G_j is a flux quantity for the convenience of analysis, q_{rj} is the net radiation flux, K_j is the extinction coefficient of the coatings and $K_j = \alpha_j + \sigma_j$, where α_j and σ_j are the absorption and scattering coefficients of the coatings, Ω_j is the scattering albedo of the coatings, and σ is the Stefan–Boltzmann constant.

To evaluate the radiation fluxes within the designed multiple layered ceramic coatings, the relationships between radiation fluxes $q^+{}_{rj}$ and $q^-{}_{rj}$ at each boundary interface are given as:

$$q_{r1}^+(\mathrm{IA}) = (1-R_0)\sigma T_1 H^4 + R_1(\mathrm{IA})q_{r1}^-(\mathrm{IA}) \tag{13}$$

$$\begin{aligned} q_{r1}^-(\mathrm{IB}) &= q_{r2}^+(\mathrm{IB}) \\ &= (1-R_2(\mathrm{IB}))q_{r2}^-(\mathrm{IB}) + R_1(\mathrm{IB})q_{r1}^+(\mathrm{IB}) \end{aligned} \tag{14}$$

$$q_{r2}^-(\mathrm{IC}) = \varepsilon_{bc} n_{\mathrm{H}}^2 \sigma T_{\mathrm{IC}}^4 + R_2(\mathrm{IC})q_{r2}^+(\mathrm{IC}) \tag{15}$$

where R_0 and $R_1(\mathrm{IA})$ are the coating reflectance of material on each side of interface IA, $R_1(\mathrm{IB})$ and $R_2(\mathrm{IB})$ are the reflectance of the material on each side of interface IB, and $R_2(\mathrm{IC})$ is the reflectance of the material on the coating side of interface IC, ε_{bc} is the emissivity of bond coat, and T_{IC} is the temperature at interface IC.

From the hot gases to the surface of the hot side of the single layer S, the heat is transferred via radiation and convection from hot gases. The convection of the hot gases brings the heat flux to the surface of the coating and increases the temperature of interface IA to T_{IA}. Part of the radiation from hot gases, incident on interface IA, is reflected by the surface IA at a reflectance of R_0, and the remaining part of the radiation is transmitted through interface IA into the coating. Therefore the total heat flux through interface IA can be expressed as the sum of the net radiation flux at the boundary and the heat flux transferred by external convection as:

$$Q_{\mathrm{tot}} = h_{\mathrm{H}}[T_{\mathrm{H}} - T_{\mathrm{IA}}] + q_{r1}(\mathrm{IA}) \tag{16}$$

where Q_{tot} is the total heat flux through the TBCs, T_{IA} is the temperature at boundary IA, and $q_{r1}(\mathrm{IA})$ is the net radiation at boundary IA.

Within the coatings, heat is transferred by conduction and radiation. Therefore, the energy equation is given by:

$$Q_{\text{tot}} = -k_j \frac{dT_j(x_j)}{dx_j} + q_{rj}(x_j) \tag{17}$$

where $j = 1$ and 2 for the single layer S and high-reflectance multiple layered stacks M, respectively, and k_j is thermal conductivity of the coatings. The radiation flux q_{rj} can be obtained from the two-flux method described.

At interface IB, the following boundary condition must be met:

$$q_{r1}(\text{IA}) = q_{r2}(\text{IB}) \tag{18}$$

On the opaque metal wall, heat is transferred only by conduction, therefore:

$$Q_{\text{tot}} = -k_3 \frac{T_{\text{ID}} - T_{\text{IC}}}{D_3} \tag{19}$$

where k_3 is the thermal conductivity of metal substrate, assuming the thermal conductivities of bond coat and metal substrate are equal, T_{IC} and T_{ID} are the temperatures at interfaces IC and ID, respectively, and D_3 is the thickness of metal substrate.

At the cooled side, the metal is cooled by convection of the cooling gas and radiation to the surroundings. Therefore, the total heat flux can be expressed as:

$$Q_{\text{tot}} = h_{\text{L}}[T_{\text{ID}} - T_{\text{IL}}] + \varepsilon_3 \sigma [T_{\text{ID}}^4 - TI_{\text{L}}^4] \tag{20}$$

where ε_3 is the metal emissivity.

Results and discussion

The temperature distribution within the coatings and the total heat flux through the TBC system are calculated by solving two-flux equations and heat transfer equations using Runge–Kutta numerical integration and iteration numerical methods. Values of numerical figures used are summarized in Table 1.

Based on the design and mathematical models described above, two different arrangements of single layer and multilayer were simulated. While the design was made to take advantage of placing the single layer S on the top layer, simulation was also conducted for a different layer arrangement. That is, placing the single layer directly on top of the bond coat and the multiple layered stacks S on the top layer. Additionally, as thickness of the single layer is a design variable, three different thicknesses for single layer are assumed, as summarized in Table 2. Furthermore, in order to demonstrate the effectiveness of the multiple layered coating designs, comparison is made by also calculating the temperature distribution in a TBC system with a mono-layered coating.

Table 1 Numerical values of various parameters used in the computation

Symbols (units)	Description	Values	Ref.
T_{H} (K)	Hot gas temperature	2000	[9]
T_{L} (K)	Cool side temperature	800	[9]
h_{H} (W m^{-2} K^{-1})	Convection coefficient	250	[9]
h_{L} (W m^{-2} K^{-1})	Convection coefficient	110	[9]
k_m (W m^{-1} K^{-1})	Thermal conductivity of metal	33	[9]
k_1 (W m^{-1} K^{-1})	Thermal conductivity of single layer S	0.8	[9]
K_2 (W m^{-1} K^{-1})	Thermal conductivity of high-reflectance multiple layered stacks M	1.5	Design variable
$D1$ (m)	Thickness of single layer S	0.0002 (A) 0.00045 (B) 0.00095 (C)	Design variable
$D2$ (m)	Total thickness of high-reflectance multiple layered stacks M	0.00005	Design variable
$D3$ (m)	Thickness of metal substrate	0.000794	[9]
n_0	Refractive index of air	1.0	[9]
n_{H}	High refractive index of high-reflectance multiple layered stacks M	2.1	[9]
n_{L}	Low refractive index of high-reflectance multiple layered stacks M and the top layer S	1.58	[9]
σ_j (m^{-1})	Scattering coefficient of ceramic material	10,000	[9]
α_j (m^{-1})	Absorption coefficient ceramic material	30	[9]
ε_{bc}	Emissivity of bond coat	0.3	[9]
ε_3	Emissivity of substrate	0.6	[9]

Table 2 Arrangement for single layer S and multiple layered stacks M (the thickness for the multiple layered stacks M is constant, with a value of 50 μm)

Model	Total thickness (μm)	Thickness of S (μm)	Description	Figures
A	250	200	Single layer is placed on the top layer, high-reflectance multiple layers are between single layer and metal	Figure 8
B	500	450	Single layer is placed on the top layer, high-reflectance multiple layers are between single layer and metal	Figure 9
C	1000	950	Single layer is placed on the top layer, high-reflectance multiple layers are between single layer and metal	Figure 10
D	250	200	High-reflectance multiple layers are on the top, single layer is between multiple layers and metal	Figure 11
E	500	450	High-reflectance multiple layers are on the top, single layer is between multiple layers and metal	Figure 12
F	1000	950	High-reflectance multiple layers are on the top, single layer is between multiple layers and metal	Figure 13

Figures 8–10 show the temperature distributions within the coating and metal substrate when a 200 μm thick single layer (Model A), 450 μm thick single layer (Model B), and 950 μm thick single layer (Model C) are used and placed above the 50 μm thick multi-layer stacks M. When the high-reflectance multiple layered stacks with the total thickness of 50 μm are used in combination with a top coat of 200 μm thick, the temperature on the metal wall can be reduced by as much as 90 °C when compared with the temperature for a system with a 250 μm mono-layered coating. The temperature reduction on the metal wall for a 500 μm multiple layered coating is about 67 °C as compared to the coating system with 500 μm mono-layered coating. It can be seen that the reduction in temperature on the metal surface becomes less pronounced with further increase in the total coating thickness, where the temperature reduction on the metal surface is only 41 °C in the case of the 1000 μm multiple layered coating (Fig. 10).

For comparison, the temperature distributions within a TBC system with multiple layered stacks placed on top of the single layer were calculated and the results are shown in Figs. 11–13. The temperature reductions are, in comparison with mono-layered coatings of the same thicknesses, 46 °C, 36 °C and 28 °C for 250 μm, 500 μm and 1000 μm thick coatings, respectively. From the results shown in Fig. 8 through Fig. 13, it is clear that the high reflectance multi-layered coating system can effectively reduce the temperature on the metal surface.

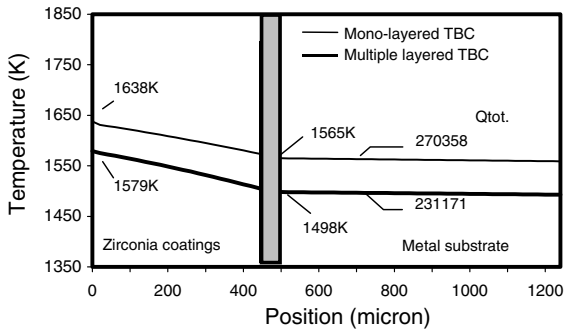

Fig. 9 Computed temperature distributions for 500 μm thick TBC within mono-layered and multiple layered coatings. The shaded area represents multiple layered coatings with 50 μm thickness

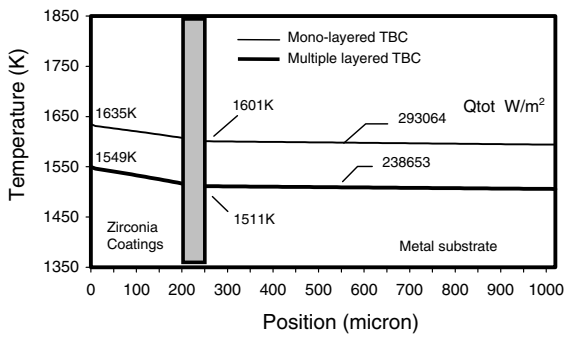

Fig. 8 Computed temperature distributions for 250 μm thick TBC within mono-layered and multiple layered coatings. The shaded area represents multiple layered coatings with 50 μm thickness

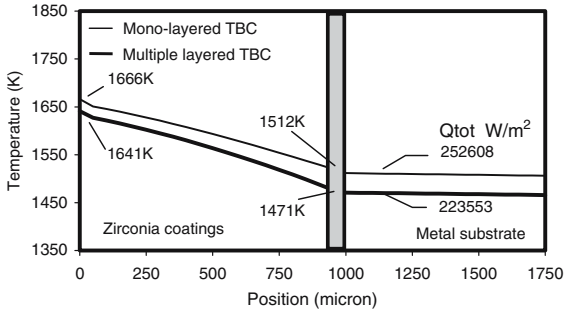

Fig. 10 Computed temperature distributions for 1000 μm thick TBC within mono-layered and multiple layered coatings. The shaded area represents multiple layered coatings with 50 μm thickness

Figs. 8 and 11 show that the temperature reduction on the metal surface is more significant when multiple layered stacks M are placed under the single layer S. It is believed that the structure with multiple layered stacks located under the single layer can reflect both external and internal radiations, whereas the structure with multiple layered stacks located on the top layer can only reflect the external radiation. In our simulation an isotropic hemispherical incident radiation on the surface is assumed for both arrangements, i.e., both have the same external radiation incident conditions. Therefore, the multiple layered stacks M, either arranged on the surface or under the layer S, is assumed to subject to isotropic hemispherical incident radiation. In fact, when the top surface is exposed to the combustion environment, radiation is near normal incident. In this case, multiple layers placed on the top of the coatings may see more near normal incidence, and the incident radiation may be more effectively reflected. Whereas if multiple layered stacks M placed under the single layer S, it may see a more hemispherical reflectance if the radiation is scattered in single S or the internal emitted radiation from the single layer is strong. In this case, the reflectivity to radiation may reduce. Thus, it will require detailed simulation to determine which arrangement can reflect radiation effectively and the reflectivity can vary depending on the materials and coating thickness selected.

It is also found that the temperature reduction on both the metal substrate and coating surface is greater for thinner multiple layered coating systems. For example, multiple layered coatings with thicknesses of 500 μm and 1000 μm are less effective in temperature reduction than is the 250 μm thick coating. With increasing coating thickness, more radiation will be absorbed by the ceramics. As such, the transmitted radiation through the coatings into the metal surface is reduced. Therefore, the overall temperature reduction effect of the thick coatings is less than that of the thin coatings.

In this simulation, the effect of coatings with nano-dimension thickness on thermal conductivity was not considered. From the theory of grain boundary phonon transport [14], the phonon mean free path is governed by the layer thickness. The thinner the coating layer thickness, the shorter the phonon mean free path. As such, the effective thermal conductivity of the high reflectance multiply layered stacks may be reduced due to the nano-dimension thickness. It can be expected, therefore, that the high-reflectance multiple layered coating system designed can reduce both photon and phonon transport through the TBC system. Further analysis using a finite element approach is being conducted at present to include the thermal conductivity reduction as a result of the nano-scaled multiple layered structure.

In contrast to the multiple layered coating design detailed in this study, a layered structure with constant layer thickness was reported by Nicholls and Lawson

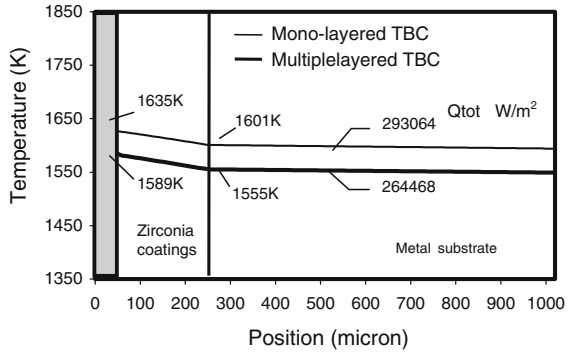

Fig. 11 Computed temperature distributions for 250 μm thick TBC within mono-layered and multiple layered coatings. The shaded area represents multiple layered coatings with 50 μm thickness

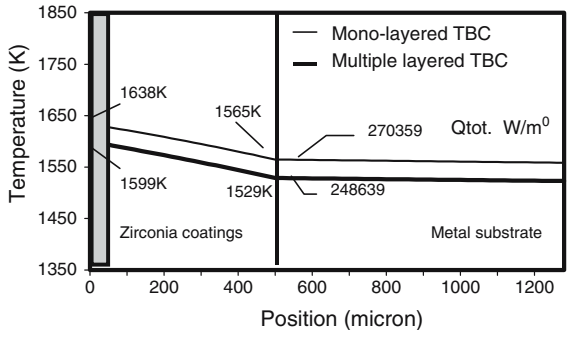

Fig. 12 Computed temperature distributions for 500 μm thick TBC within mono-layered and multiple layered coatings. The shaded area represents multiple layered coatings with 50 μm thickness

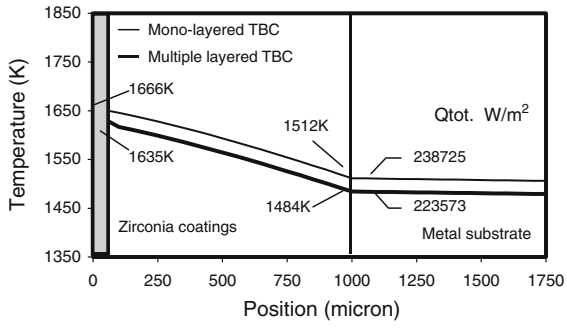

Fig. 13 Computed temperature distributions for 1000 μm thick TBC within mono-layered and multiple layered coatings. The shaded area represents multiple layered coatings with 50 μm thickness

[10]. This type of layered structure is limited to reflecting one wavelength range, while the present design is designed to reflect a wide range of wavelengths. The physical thicknesses of the high reflectance multiple layered structures in the present design are tailored for different wavelength ranges so that broadband thermal radiation can be reflected, achieving far more effective thermal radiation reduction.

In the design and simulation, all the material properties used are based on ceramics such as zirconia and YSZ co-doped with other oxides. The use of metal interlayers is excluded in this multiple layered coating design since the thermal expansion mismatch between metal and ceramics could potentially cause interface delamination or the formation of detrimental phases in the interface in the harsh operating environment.

In addition to the temperature drop on the metal surface, the temperatures on the coating surface are reduced significantly when the multiple layered coating system is used. For example, in model A, the 250 μm multiple layered coating could reduce the coating surface temperature by about 90 °C. This will increase the thermal stability for conventional ceramic materials such that higher operating temperatures can be realized.

Lastly, it is generally agreed that in order to produce multiple beam interference effect, i.e., coherent constructive reflection, the multiple layered stacks M are required to have a very low scattering coefficient. It is also known that the low scattering requires a dense defect-free coating structure. For a compliant TBC coating, columnar structure produced by EB-PVD is preferred. This columnar structure inherently contains multiple defects along columnar boundaries and within columns. As such, the scattering coefficient for this type of strain tolerant columnar structure will increase in comparison to defect free single crystal structure. The resulted multiple beam interference effect will be compromised accordingly. However, as shown in Fig. 14 [15], the multiple beam interference effect is still clearly observed at wavelength of 2 μm. Since this multiple layered EB-PVD coating structure is not optimally designed, the interference effect can be further increased using the approach detailed in this study.

It is believed that the coating structure can be designed in such a way that it contains adequate amount of defects to accommodate strain imposed on coating during service while at the same time to achieve the desirable reflectance. The actual reflectivity of this multiple layered coating design may be reduced from the theoretically calculated values due partially to the scattering effect. Further experiment is being conducted to assess the extent of this effect.

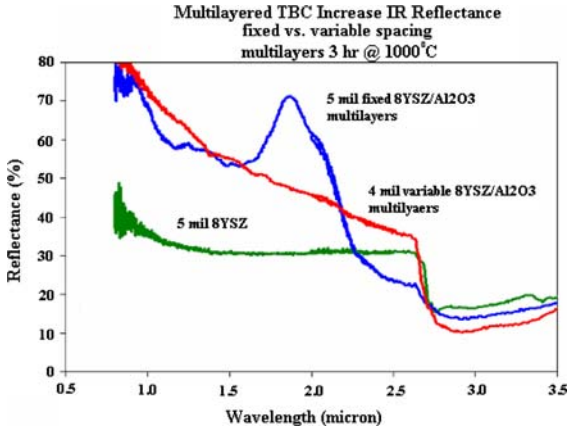

Fig. 14 Hemispherical reflectance of nanolayered coatings composed of 8YSZ/Al_2O_3 produced by co-evaporation of two ingots simultaneously in the EB-PVD chamber [15]

Various material combinations and process parameters will be used to produce the designed multiple layered structures. The coating structures will then be tested for their physical properties and thermal mechanical properties. At the same time, further theoretical modeling is being conducted to quantitatively evaluate the effect of scattering at different levels. Until such time when both experiment results and detailed analysis on scattering effect are obtained, it is difficult to speculate the feasibility of multiple layered structures with high reflectance.

Conclusion

In this study, a multiple layered TBC coating system was designed and a mathematical simulation was carried out to compute the temperature distribution on the metal and coating surfaces as a result of applying this designed multiple layered coating. From the simulation results, it is concluded that the multiple layered TBC system, based solely on ceramic materials, can achieve greater than 50% reflectance of the radiation in the wavelength range of 0.45–5 μm. The simulation conducted uses the published data on physical and optical properties of the known TBC materials. While an acceptable deposition technique for applying such a variable layer thickness coating is being developed, the effectiveness of this model will be validated once experimental data is available. Nevertheless, this design has shown promising results and indicates great potential for further temperature reduction on the metal surface.

Acknowledgements The authors would like to thank the Natural Science and Engineering Research Council of Canada for

providing financial support for this research. The author (Dongmei Wang) would also like to thank Carleton University for supporting her with a fellowship and teaching assistantship.

References

1. Klemens PG (1999) Physica B 263–264:102
2. Rickerby DS (1998) European Patent EP 0 825 271 A1
3. Gu S, Lu TJ, Hass DD, Wadley HNG (2001) Acta Mater 49:2539
4. Brandon JB, Taylor R (1991) Surf Coat Technol 46:75
5. Schulz U (2000) J Am Ceram Soc 83(4):904
6. Fritscher K, Szucs F, Schulz U, Saruhan B, Peters M, Kaysser WA (2002) Ceramic Eng Sci Proc 23(4):341
7. Vassen R (2000) J Am Ceram Soc 83(8):2023
8. Eldridge JI, Spuckler CM, Street KW (2002) Infrared Radiative Properties of Yttria-Stabilized Zirconia Thermal Barrier Coatings, 26th Annual Conference of Composites, Advanced Ceramics, Materials and Structures: B, Cocoa Beach, FL, Jan 13–18, 2002. American Ceramic Society, Westerville, OH, p 417
9. Siegel R, Spuckler CM (1998) Mater Sci Eng A245:150
10. Nicholls JR, Lawson KJ (2001) Mater Sci Forum 369–372:595
11. Allen WP (2003) Reflective Coatings to Reduce Radiation Heat Transfer, US patent US 0008170 A1
12. Siegel R, Howell JR (December 15, 2001) Thermal radiation heat transfer, 4th edn. Taylor & Francis
13. Macleod HA (1986) Thin-film optical filters, 2nd edn. Published by Adam Hiller Ltd., pp 158–186
14. Klemens PG (1997) In: Ma E, Fultz B (eds) Theory of thermal conductivity of nanophase material, chemistry and physics of nanostructures and related non-equilibrium materials. The Minerals, Metals & Materials Society
15. Singh J, Wolfe DE (2005) J Mater Sci 40:1